

Double photoexcitation of He atoms by attosecond xuv pulses in the presence of intense few-cycle infrared lasers

X. M. Tong* and C. D. Lin

J. R. Macdonald Laboratory, Physics Department, Kansas State University, Manhattan, Kansas 66506, USA

(Received 2 December 2004; published 10 March 2005)

We studied the photoelectron spectra of He atoms resulting from double photoexcitation to autoionizing states by an attosecond xuv pulse in the presence of intense few-cycle Ti:sapphire lasers using the time-dependent hyperspherical close-coupling method. In its first application we show that the combination of a weak xuv pulse and an intense infrared laser offers an efficient means for probing states that cannot be reached by single photoabsorption experiments alone. The method provides an alternative approach of studying Stark induced states at field strength much higher than that available for a dc electric field. Using parameters from the presently available attosecond pulses and infrared lasers we showed that the four singlet $2\ell 2\ell'$ doubly excited states of He are prominently excited in such experiments. The dependence of the shape of the autoionizing states thus generated has been studied with respect to the intensity and the carrier-envelope phase of the few-cycle laser pulses.

DOI: 10.1103/PhysRevA.71.033406

PACS number(s): 42.50.Hz, 32.80.Rm, 33.80.Eh

I. INTRODUCTION

Single attosecond xuv or soft x-ray pulses by high-order harmonic generation from rare-gas atoms with few-cycle femtosecond lasers have been reported recently [1,2]. The attosecond time scale is comparable to the typical time scale of electronic interactions inside an atom or a molecule where the periods of the electronic motion or the transition times are of the order of hundreds of attoseconds or a few femtoseconds. With such attosecond pulses, they can be used to probe the electronic motion, or to steer the electronic transitions, i.e., to perform coherent control of electrons, akin to femtosecond or picosecond lasers in controlling atomic motion in molecules. For instance, the inner-shell holes, or the autoionizing states of atoms, molecules, or solids, in general, have lifetimes of fractions to several femtoseconds. In fact, in a proof-of-principle experiment with attosecond pulses, the Auger lifetime of an inner-shell hole of Krypton has been determined [3] in the time domain. The result of about 8 fs is in good agreement with the lifetime deduced from the Auger width measured by the traditional high-precision Auger electron spectroscopy.

When electrons in an atom or molecule are excited, there are various periodic motions, or modes, where the periods are of the order of hundreds of attoseconds or a few femtoseconds. For example, if one can excite the ground state and the $2p$ excited state of atomic hydrogen coherently, the electron is expected to perform dipole oscillations with periods of a few hundreds attoseconds. Such measurements would be just another proof-of-principle experiment. It would not offer exciting new understanding on electron dynamics in an atom.

As the technology of attosecond light pulses becomes more mature, a far-reaching goal would be to identify problems which cannot be probed by other means. In particular, motions involving electronic interactions are in the sub-fs

time scale. In the energy domain measurements, the effects of electron-electron interactions are averaged over long time. The result of this average is described very loosely as electron correlation. In other words, in energy domain measurements the dynamics of electron-electron interactions is completely missing. Only attosecond technology can probe, and later, steer, the dynamics of the interactions between the electrons.

The study of electron-electron interaction dynamics will be challenging. For atoms, it is known that the motion of individual electrons is mostly governed by its Coulomb interaction with the nucleus. The effect of the other electrons is relatively weak and can first be approximated by screening. For such situations, it is difficult to observe pronounced features that characterize the electron-electron interaction dynamics. In the energy domain, this belongs to classes of experiments where electron correlation can be treated perturbatively. Fortunately, there are situations where electron-electron correlation plays major roles in atoms and molecules—these are multiply excited states where two or more electrons are excited simultaneously. The simplest of multiply excited states are the doubly excited states of a helium atom where both electrons are excited.

Doubly excited states of helium were first systematically studied experimentally in the early 1960's when synchrotron radiation became available [4]. Starting with the ground state, absorption of a photon with energies near 60 eV can populate 1P doubly excited states, such as $2snp$, $2pns$, or $2pnd$, according to the shell-model picture. In this designation, for example, for $2snp$, this implies that one electron is in the $2s$ state and the other in the np state. However this shell-model picture is inconsistent with the experimental results from Madden and Codling [4]. It was argued by Fano and co-workers [5] that a better description of these doubly excited states be expressed as $2snp+2pns$, $2snp-2pns$, and $2pnd$ series, later called “+,” “-,” and pd series, respectively. Only states in the “+” series are predominantly excited by the photons.

*Contact: xmtong@phys.ksu.edu

The “+” and “−” designation of doubly excited states, in fact, has a much deeper significance. It describes the joint motion of the two electrons explicitly, instead of the motion of individual electrons as in the shell model. In analogy to the mechanical motion of two coupled springs, the pair of electrons in the “+” states performs in-phase oscillations where the two electrons approach or recede from the nucleus together. For the “−” states, the oscillation is out-of-phase where one electron approaches the nucleus while the other is moving away, and vice versa. The effect of these in-phase or out-of-phase motions between the two electrons is reflected by their drastically different decay lifetimes and photoabsorption probabilities. With attosecond pulses, such in-phase and out-of-phase motion probably can be probed directly in the time domain. Besides these radial stretches of the two electrons, the two electrons in doubly excited states can also execute bending vibrations, where the angle of the two electrons with respect to the nucleus can be approximated by bending vibrational quantum numbers. These modes are expected to have periods of the order of sub-fs to a few femtoseconds as well.

Many theoretical models [6–10] have studied such internal modes of the joint motion between the two electrons for doubly excited states. Still the main question is how such modes can be revealed in actual experiments? Existing experiments involving attosecond light pulses used xuv-pump and few-cycle laser probe technique where photoelectrons generated by the xuv pulse are steered in the laser field for different time delays between the two pulses. How can the internal stretching and bending modes between the two electrons be probed using such a technique and how would the electron spectra reveal such modes? In the absence of experimental data, it is desirable to perform theoretical simulations by solving the time-dependent Schrödinger equation directly for guidance.

Direct solution of the time-dependent Schrödinger equation for helium atoms in an intense laser field has been reported by a number of groups [11–14]. These calculations focused on the double ionization cross sections by the intense lasers. For the present purpose, it is essential that the equation be solved accurately such that doubly excited states are well described. In this paper, we present the theoretical method we have developed based on propagating the time-dependent wave function in hyperspherical (HS) coordinates. In the HS system, there is only one radial coordinate—the hyperradius R , thus the calculation can be confined to a large hypersphere with some cutoff radius, analogous to what one would do for a one-electron system. To test that the method can indeed accurately describe the atomic structures, including doubly excited states, we have applied the method in an earlier paper where we calculated the energies and widths of doubly excited states formed from photoabsorption in an intense static dc electric field. With the highest electric field of the order of 100 kV/cm, many interesting Stark induced doubly excited states were observed in the experiment of Harries *et al.* [15]. However, such dc Stark effect can probe the $n=6$ and 7 doubly excited states ($N\ell n\ell'$) below the $N=2$ threshold of He^+ only. To study the Stark effect of the $2\ell 2\ell'$ intrashell states, the needed high static electric field is not available. As another test of the theoretical method, in

this paper we suggest an experiment to study intrashell doubly excited states of He in the combined field of an attosecond xuv pulse and an intense laser pulse with peak intensity of the order of $I_0=10^{12}$ W/cm². This would correspond to electric field of about 10^7 V/cm, two orders higher than the available dc electric field.

While the present suggested experiment does not exploit the attosecond nature of the xuv pulse, such studies are very important in order to test the theoretical and experimental tools under development. The attosecond xuv pulse is used here not only to provide a broad band of photon energies, but also a sharp start time where doubly excited states are first formed. With the introduction of an intense few femtosecond laser pulses overlapping with the attosecond xuv pulses, the autoionization process can be modified at the control of the experimentalist, through the change in laser intensity, pulse length, and the time delay between the two pulses. Since the xuv light and the laser are coherently related, the carrier envelope phase will play a crucial role in determining the electron spectra. With the many knobs available to tune, it is hoped that the dynamics between two electrons, including the autoionization itself, can be probed and eventually controlled in the future.

II. THEORETICAL METHOD

Generally speaking, the dynamics of a two-electron helium atom in the external field can be studied by solving the following time-dependent Schrödinger equation (in atomic units $m=\hbar=e=1$)

$$i\frac{\partial}{\partial t}\Psi(\mathbf{r}_1, \mathbf{r}_2, t) = [H_0(\mathbf{r}_1, \mathbf{r}_2) + V_{ext}(t)]\Psi(\mathbf{r}_1, \mathbf{r}_2, t), \quad (1)$$

with

$$H_0(\mathbf{r}_1, \mathbf{r}_2) = -\frac{\nabla_1^2}{2} - \frac{2}{r_1} - \frac{\nabla_2^2}{2} - \frac{2}{r_2} + \frac{1}{|\mathbf{r}_1 - \mathbf{r}_2|}, \quad (2)$$

where the wave function is expanded as

$$\begin{aligned} \Psi(\mathbf{r}_1, \mathbf{r}_2, t) = & \frac{1}{r_1 r_2} \left(\sum_{i, l_1 \neq l_2} [f_i(r_1, r_2, t) Q_{LM}(l_1, l_2) \right. \\ & \left. + (-1)^A f_i(r_2, r_1, t) Q_{LM}(l_2, l_1)] \right. \\ & \left. + \sum_{j, l_1 = l_2} f_j(r_1, r_2, t) Q_{LM}(l_2, l_1) \right). \quad (3) \end{aligned}$$

Here

$$A = l_1 + l_2 + L + S,$$

$$Q_{LM}(l_1, l_2) = \sum_{m_1, m_2} \langle l_1 m_1 l_2 m_2 | LM \rangle Y_{l_1 m_1}(\hat{\mathbf{r}}_1) Y_{l_2 m_2}(\hat{\mathbf{r}}_2).$$

Here, i stands for the collection of quantum numbers $LM(l_1, l_2)$. $V_{ext}(t)$ is the interaction between the electrons and the external time-dependent field. Directly solving the above equation is still a challenge for the present supercomputers. We will focus on a laser-assisted photoionization process involving only single ionization and doubly excited states. In

such a case, we can solve the above equation using the hyperspherical close-coupling method. In hyperspherical coordinates, we define

$$R = \sqrt{r_1^2 + r_2^2}, \quad (4)$$

$$\tan \phi = \frac{r_1}{r_2}, \quad (5)$$

$$f_i(r_1, r_2, t) = \sum_{\alpha} F_{\alpha}^L(R, t) \Omega_{\alpha}^L(R, \phi, i) / \sqrt{R}. \quad (6)$$

Now, the total wave function can be expressed as

$$\begin{aligned} \Psi(R, \phi, \hat{\mathbf{r}}_1, \hat{\mathbf{r}}_2, t) &= \frac{1}{R^{5/2} \cos \phi \sin \phi} \sum_{\alpha, L} F_{\alpha, L}^L(R, t) \times \sum_i \begin{cases} \frac{1}{\sqrt{2}} [\Omega_{\alpha}^L(R, \phi, i) Q_{LM}(l_1, l_2) + (-1)^A \Omega_{\alpha}^L(R, \pi/2 - \phi, i) Q_{LM}(l_2, l_1)], & l_1 \neq l_2 \\ \Omega_{\alpha}^L(R, \phi, i) Q_{LM}(l_1, l_2), & l_1 = l_2 \end{cases} \\ &= \frac{1}{R^{5/2} \cos \phi \sin \phi} \sum_{\alpha, L} F_{\alpha, L}^L(R, t) \bar{\Omega}_{\alpha}^L(R, \phi). \end{aligned} \quad (7)$$

If we discretize R by a pseudospectral method, we can further write

$$\sum_{\alpha} F_{\alpha}^L(R, t) = \sum_{\alpha} C_j^{L, \alpha}(t) g_j(R), \quad (8)$$

with $g_j(R)$ being the pseudospectral basis function. If we choose $\{R_j\}$ as the set of canonical coordinates, then

$$g_j(R_{j'}) = \begin{cases} 1 & j = j' \\ 0 & j \neq j' \end{cases}. \quad (9)$$

With the pseudospectral basis, we can rewrite Eq. (1) as

$$\begin{aligned} i \frac{\partial}{\partial t} C_j^{L, \alpha}(t) &= \sum_{\alpha', j'} T_{j, j'} S_{j, j'}^{\alpha, \alpha'} C_{j'}^{L, \alpha'}(t) + U_{\alpha}^L(R_j) C_j^{L, \alpha}(t) \\ &+ E(t) \sum_{L', \alpha'} D_{\alpha, \alpha'}^{L, L'}(R_j) C_j^{L', \alpha'}(t). \end{aligned} \quad (10)$$

Here

$$T_{j, j'} = \left[-\frac{1}{2} \frac{d^2}{dR^2} \right]_{j, j'}, \quad (11)$$

$$S_{j, j'}^{\alpha, \alpha'} = \int_0^{\pi/2} \bar{\Omega}_{\alpha}^L(R_j, \phi) \bar{\Omega}_{\alpha'}^L(R_{j'}, \phi) d\phi, \quad (12)$$

$$\begin{aligned} D_{\alpha, \alpha'}^{L, L'}(R) &= \int \bar{\Omega}_{\alpha}^L(R, \phi) \mathbf{D} \bar{\Omega}_{\alpha'}^{L'}(R, \phi) d\phi \\ &= R \int \bar{\Omega}_{\alpha}^L(R, \phi) (\sin \phi \cos \theta_1 \\ &+ \cos \phi \cos \theta_2) \bar{\Omega}_{\alpha'}^{L'}(R, \phi) d\phi. \end{aligned} \quad (13)$$

$U_{\alpha}^L(R_j)$ is the eigenenergy at fixed R_j and channel α . Note that in the above equations, only $C_j^{L, \alpha}(t)$ depends on time. All the other quantities do not depend on time and can be calcu-

lated once for all. The nonadiabatic couplings between the channels are treated by the smooth-variable-discretization (SVD) method developed by Tolstikhin *et al.* [16]. The adiabatic potential curves $U_{\alpha}^L(R)$ and the channel functions $\bar{\Omega}_{\alpha}^L(R, \phi)$ are obtained by solving the coupled equations in ϕ . The time propagation is performed by the generalized time-dependent pseudospectral method in the energy representation [17]. Here we chose $R_{\max} = 1000$ a.u. to avoid the need of worrying about reflections from the boundaries. Both the xuv and laser pulses are so short that the field is well over before the ionization wave packet reaches the boundary. The photoionization probability is extracted by the R -matrix method [18].

If we choose the initial state as the ground state of He and the external field is a combination of attosecond pulse and an ultrashort laser field,

$$E(t) = E_x e^{-(2 \ln 2) t^2 / \tau_x^2} \cos(\omega_x t) + E_l e^{-(2 \ln 2) t^2 / \tau_l^2} \cos(\omega_l t + \delta), \quad (14)$$

we can calculate the transition probability $P(\omega)$ from the ground state to the single ionization and to doubly excited states. Here δ is the carrier envelope phase. To compare with the conventional photoionization cross section, we define an effective photoionization cross section by

$$\sigma(\omega) = \frac{4\pi^2 \omega P(\omega)}{c A(\omega)}, \quad (15)$$

$$A(\omega) = \frac{\pi \tau_x^2 E_x^2}{4} \left(e^{-\tau_x^2 (\omega - \omega_x)^2 / 4} + e^{-\tau_x^2 (\omega + \omega_x)^2 / 4} \right)^2.$$

III. RESULTS

A. xuv photoionization with and without the laser field

The time-dependent hyperspherical close-coupling method outlined above allows us to calculate the photoelec-

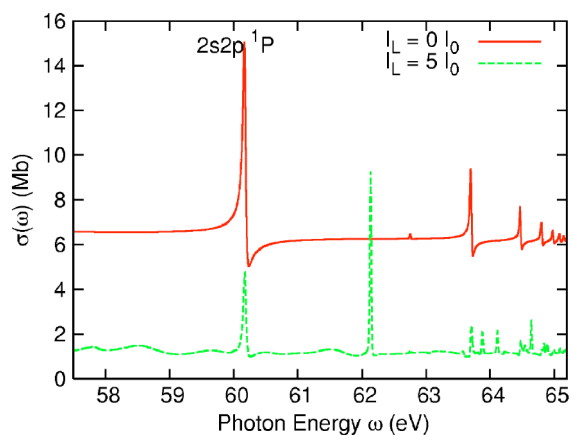


FIG. 1. (Color online) The He photoionization cross section with or without the laser fields. For better visualization, we upshift the field-free cross section by 5 Mb. The laser intensity is in the unit of $I_0=10^{12}$ W/cm².

tron spectra of He atoms in a short xuv pulse, with or without the presence of an intense infrared laser field. Here we chose the xuv pulse duration full width at half maximum $\tau_x=0.2$ fs, with central photon energy $\omega_x=60.0$ eV. The laser pulse duration is taken at $\tau_l=5.0$ fs, with central wavelength at 800 nm. In the actual simulation, we choose the xuv intensity $I_x=10^{12}$ W/cm². Note that the cross section does not depend on the xuv intensity.

To test the accuracy of the theoretical method, we first turn off the laser field and propagate the time-dependent wave function for a long time before it reaches the boundary. The calculated photoionization cross sections, from Eq. (15), as shown in Fig. 1, are in good agreement with our own calculations carried out using the time-independent method. The latter are in good agreement with other theoretical calculations and with the high-resolution photoabsorption data of He from Domke *et al.* [19]. In this spectra, the first peak has been labeled using the conventional notation, as the $2s2p\ ^1P^o$ state. The pronounced series of peaks are the higher members of the “+” series. The small bump slightly below 63 eV is the first member of the “-” series, or the $(2s3p-2p3s)\ ^1P^o$ state. Note that we plot the spectra in terms of photon energies for convenient comparison with high-resolution photoabsorption measurements. For the 0.2-fs xuv pulses used here, the photon energy covers a broad band, thus what is measured is actually the electron energy.

We next turn on the laser field. From the lower curve in Fig. 1 we note that many additional resonances or doubly excited states are induced when a laser of intensity of $5 I_0$ is added on top of the attosecond xuv pulse (no time delay between the two). The electron spectra (but shown in terms of equivalent photon energies) are analogous to the photoabsorption spectra of He in a static electric field, except that the highest static electric field that can be reached for such experiments is of the order of 10^5 V/cm [15]. At such fields, the Stark effect can be seen only for the higher ($n=6,7$) Rydberg states [15,20]. On the other hand, even for a moderate laser intensity of $5 I_0$ ($I_0=10^{12}$ W/cm²), the peak electric field is already 6×10^7 V/cm, nearly three orders of

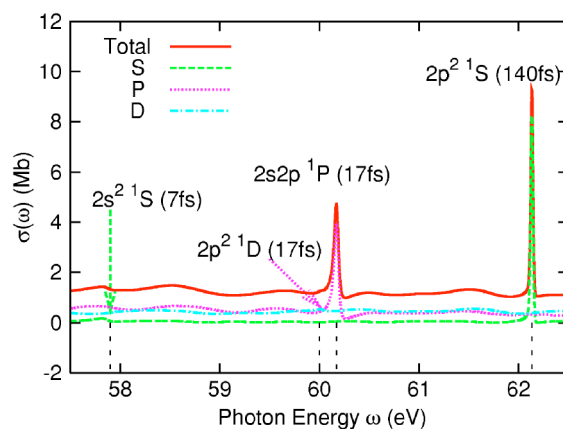


FIG. 2. (Color online) Laser assisted photoionization cross section of He decomposed into different total angular momenta. The laser intensity is $5 I_0$ and $\delta=0$. The vertical dashed lines show the energy positions of the four singlet doubly excited states of $2\ell 2\ell'$.

magnitude higher than the laboratory static dc field. Thus it is relatively easy to observe new resonances if the photoabsorption of xuv pulse is performed in the presence of a moderate intense laser pulse. This type of Stark effect has not been addressed previously in the simplified laser-assisted photoionization theory based on the strong-field approximation so far [21,22].

In Fig. 2 we analyze the spectral range of 58–62 eV where intrashell $2\ell 2\ell'$ doubly excited states of He are located. We decompose our calculated photoelectron spectra in terms of partial wave contributions. The laser intensity is $5 I_0$ with 5-fs pulse duration. Note that such a short pulse laser is already available [23]. Different from the conventional photoionization spectra, due to the presence of the laser, we also can observe the 1S and 1D and other higher angular momentum states. In the present simulation, the continuum background mainly transferred to the D channel. The S channel has less contributions apart from the new resonances. As a matter of fact, the sharp peak around 62 eV comes from $2p^2\ ^1S$. Since this state has the longest lifetime (140 fs) among the $2\ell 2\ell'$ states, this resonance is very sharp. The Auger lifetime of $2s^2\ ^1S$ is 7 fs, which is comparable to the laser pulse duration (5 fs). Thus it is not easy to observe the resonance structure of this state. The resonance position of $2p^2\ ^1D$ is very close to the laser-free $2s2p\ ^1P$ peak so it is also difficult to resolve it.

A few words about the calculations. To ensure convergence we have chosen the maximum total orbital angular momentum L up to 9 and for each L , the hyperspherical channels below the $N=1$ and $N=2$ limits of He⁺ are included. For less accurate calculations, the channels included can be significantly reduced. They were added here to explore the computational needs of the method. For example, for the calculations described above, each calculation takes about 24 h on moderate supercomputers. The advantage of this method is that with one calculation, we can obtain the whole spectra.

B. Laser intensity dependence

In Fig. 3 we show the dependence of laser-assisted photoelectron spectra on the intensity of the laser. All the param-

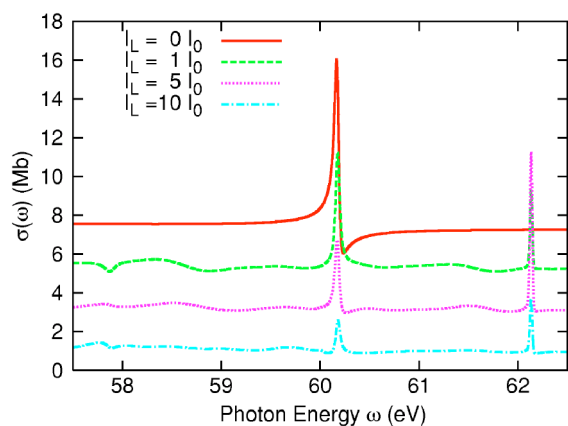


FIG. 3. (Color online) Laser-assisted photoionization cross section of He with laser intensities at 0, 1, 5, and 10 I_0 , respectively.

eters are the same as in Fig. 2 except that the peak laser intensity has been varied from 0 to 1, 5, and 10 I_0 . In the 57–63-eV photon energy region, the presence of the $2p^2\ ^1S$ state is most prominent. Its sharp structure is due to its long lifetime. Its Lorentzian shape again is a consequence of its long lifetime—the state decays long after the laser and xuv pulses are over and thus there is little interference with the continuum. On the other hand, the Stark field induced $2s^2\ ^1S$ resonance is broader and appears to be weaker. It exhibits windowlike Fano resonance shape and the shape varies with the laser intensity. This is the result of general interference and of its short lifetime, thus it decays in the presence of the driving laser field.

From the analysis of the calculation, the $2p^2\ ^1D$ resonance is clearly populated as well. Since it is very close to the $2s2p\ ^1P$ state its features cannot be clearly seen in the figure. Careful observation of Fig. 3 also shows that the oscillator strength of the $2s2p\ ^1P$ decreases with increasing laser intensity, as its strength is being shared by the other states. The laser intensity has been chosen such that direct ionization from the ground state by the laser is negligible such that the total oscillator strength by the xuv pulse is just redistributed with the resonances as well as the “continuum” electrons.

C. Carrier-envelope phase dependence

For the short laser pulses at 5 fs the carrier-envelope phase, or simply the carrier phase, is important. In combining the xuv pulse with the few-cycle laser pulses, different carrier phases would give different combined electric fields. Figure 4 shows the laser-assisted photoionization spectra for different carrier envelope phase δ . Increasing the carrier phase is equivalent to reducing the instantaneous dc field strength at the peak of the x-ray pulse. Thus the $2p^2\ ^1S$ peak strength also decreases. Meanwhile, as we increase the carrier phase, the drift velocity also increases (recall the drift velocity is 90° out of phase with respect to the electric field), which will transfer more of the oscillator strength of the $2s2p\ ^1P$ to other channels. Thus the peak strength of this state decreases as the carrier phase increases. The largest increase is for the 90° carrier phase where the $2p^2\ ^1D$ state can be observed. The calculation also shows that the shape of

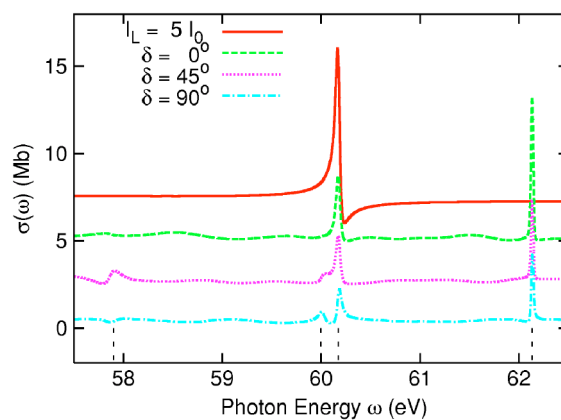


FIG. 4. (Color online) Dependence of laser-assisted photoionization cross section of He on the carrier envelope phase of the laser. The laser intensity is 5 I_0 . The vertical dashed lines show the energy positions of the four singlet doubly excited states of $2\ell 2\ell'$.

the $2s^2\ ^1S$ resonance changes drastically depending on the carrier phase—again a consequence of its short lifetime and that the drift velocity from the laser field depends critically on the carrier phase of the laser pulse.

IV. SUMMARY AND CONCLUSIONS

In this paper we described a different method of solving the time-dependent Schrödinger equation for a two-electron atom in a combined xuv pulse and an intense few-cycle laser. The two-electron wave function is expressed in hyperspherical coordinates. Our eventual goal is to study pump-probe-type experiments where the electron-electron interaction dynamics can be examined at hundreds of attoseconds resolution. In an earlier paper [20] we have tested the numerical accuracy of our approach by studying the $2\ell n\ell'$ ($n=6,7$) doubly excited states of He in a strong dc electric field. That study confirmed that the atomic structure of doubly excited states can be accurately calculated using the hyperspherical method. In the present paper, we performed the more demanding calculations by directly integrating the two-electron time-dependent Schrödinger equation. As a first application, we studied the $2\ell 2\ell'$ resonances of He populated in a combined attosecond xuv pulse and a few-cycle Ti-sapphire laser. We investigated how the electron spectra and the strength and shape of the Stark field induced resonances depend on the laser intensity and the carrier phase of the few-cycle laser. While the present study did not take advantage of the time structure of the attosecond xuv pulses, we are ready to perform *ab initio* calculations to study the electron-electron dynamics involving doubly excited states where electron correlation is known to play a major role from the energy-domain studies.

ACKNOWLEDGMENT

This work was supported in part by the Chemical Sciences, Geosciences and Biosciences Division, Office of Basic Energy Sciences, Office of Science, U. S. Department of Energy.

- [1] M. Drescher, M. Hentschel, R. Kienberger, G. Tempea, C. Spielmann, G. A. Reider, P. B. Corkum, and F. Krausz, *Science* **291**, 1923 (2001).
- [2] Z. Chang, *Phys. Rev. A* **70**, 043802 (2004).
- [3] R. Kienberger, M. Hentschel, C. Spielmann, G. A. Reider, N. Milosevic, U. Heinzmann, M. Drescher, and F. Krausz, *Appl. Phys. B: Lasers Opt.* **74**, S3 (2002).
- [4] R. P. Madden and K. Codling, *Phys. Rev. Lett.* **10**, 516 (1963).
- [5] J. W. Cooper, U. Fano, and F. Prats, *Phys. Rev. Lett.* **10**, 518 (1963).
- [6] D. R. Herrick, *Adv. Chem. Phys.* **52**, 1 (1983).
- [7] C. D. Lin, *Phys. Rev. A* **29**, 1019 (1984).
- [8] C. D. Lin, *Adv. At. Mol. Phys.* **22**, 77 (1986).
- [9] J. M. Feagin and J. S. Briggs, *Phys. Rev. A* **37**, 4599 (1988).
- [10] J. M. Rost, K. Schulz, M. Domke, and G. Kaindl, *J. Phys. B* **30**, 4663 (1997).
- [11] J. Parker, K. T. Taylor, C. W. Clark, and S. Blodgett-Ford, *J. Phys. B* **29**, L33 (1996).
- [12] D. Bauer, *Phys. Rev. A* **56**, 3028 (1997).
- [13] M. Taut, A. Ernst, and H. Eschrig, *J. Phys. B* **31**, 2689 (1998).
- [14] N. E. Dahlen and R. van Leeuwen, *Phys. Rev. A* **64**, 023405 (2001).
- [15] J. R. Harries, J. P. Sullivan, J. B. Sternberg, S. Obara, T. Suzuki, P. Hammond, J. Bozek, N. Berrah, M. Halka, and Y. Azuma, *Phys. Rev. Lett.* **90**, 133002 (2003).
- [16] O. I. Tolstikhin, S. Watanabe, and M. Matsuzawa, *J. Phys. B* **29**, L389 (1996).
- [17] X. M. Tong and S. I. Chu, *Chem. Phys.* **217**, 119 (1997).
- [18] D. Kato and S. Watanabe, *Phys. Rev. A* **56**, 3687 (1997).
- [19] M. Domke, G. Remmers, and G. Kaindl, *Phys. Rev. Lett.* **69**, 1171 (1992).
- [20] X. M. Tong and C. D. Lin, *Phys. Rev. Lett.* **92**, 223003 (2004).
- [21] M. Kitzler, N. Milosevic, A. Scrinzi, F. Krausz, and T. Brabec, *Phys. Rev. Lett.* **88**, 173904 (2002).
- [22] Z. X. Zhao and C. D. Lin, *Phys. Rev. Lett.* (to be published).
- [23] A. Apolonski *et al.*, *Phys. Rev. Lett.* **92**, 073902 (2004).